Crystal field energy levels of Eu^{3+} and Yb^{3+} in the C_2 and S_6 sites of the cubic C-type R_2O_3

Crystal field energy levels of Eu^{3+} and Yb^{3+} in the C_2 and S_6 sites of the cubic C-type R_2O_3

Elisabeth Antic-Fidancev[1,3]**, Jorma Hölsä**[2] **and Mika Lastusaari**[2]

[1] Laboratoire de Chimie Appliquée de l'État Solide, UMR-7574, CNRS, ENSCP, 11, rue Pierre et Marie Curie, F-75231 Paris Cédex 05, France
[2] Laboratory of Inorganic Chemistry, Department of Chemistry, University of Turku, FIN-20014 Turku, Finland

E-mail: antic@ext.jussieu.fr

Abstract

In the cubic C-type rare-earth (R) sesquioxides, C-R_2O_3, the trivalent R ions (R^{3+}) occupy two different crystallographic sites with S_6 and C_2 symmetries. The R ions in the C_2 lattice site have been studied intensively whereas the properties of the R^{3+} ions in the S_6 site are largely unknown or the data are contradictory. Based on the spectroscopic data reinterpreted by a phenomenological crystal field (cf) analysis a new interpretation was obtained for the energy level scheme of the Eu^{3+} ions in the S_6 site of C-R_2O_3. The cf parameters obtained were then used to predict the energy level scheme of the Yb^{3+} ion in the same host lattices. In the prediction, the evolution of the cf parameters along the R series studied earlier in the R oxide and garnet systems was used. The relationship between the cf strength parameter and the overall splitting of the $^{2S+1}L_J$ levels as well as the relationship between the barycentres of the free ion levels were used, also, to reinterpret the energy level scheme of the Yb^{3+} ion in the C_2 site of C-Y_2O_3.

1. Introduction

The diode-pumped solid-state (tunable) laser (DPSSL) systems based on Yb^{3+}-doped materials are being studied intensively at the moment [1]. The potential host lattices considered for this promising pseudo-three-level lasing system include simple or complex oxide, garnet, borate, silicate, and tungstate systems [1–8]. The cubic C-type rare-earth (R) sesquioxides, C-R_2O_3, are other possible host compounds due to their wide transparency in the wavelength range involved, around 1000 nm. The C-R_2O_3 host lattice can easily be doped with R^{3+} ions which usually exhibit high luminescence efficiency. Some materials (e.g. Y_2O_3:Eu^{3+}) have found

---

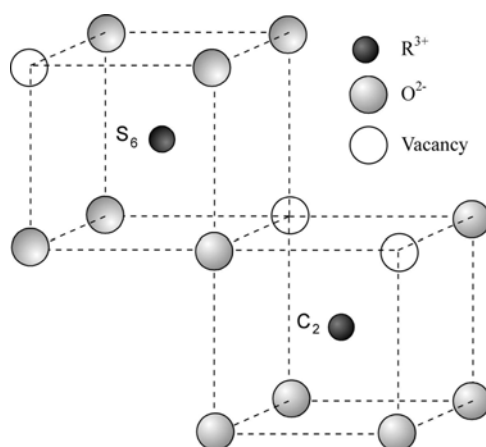[3] Author to whom any correspondence should be addressed.

Figure 1. A schematic presentation of the R^{3+} coordination in the C_2 and S_6 sites of cubic C-Y_2O_3.

commercial applications, e.g. as the red-emitting phosphor in low-pressure mercury fluorescent tubes [9]. For the laser application, in addition to the high luminescence efficiency, high heat conductivity is needed to dissipate the heat due to pumping. The heat conductivity of C-Y_2O_3 is higher than that of the classical laser material, yttrium aluminium garnet (YAG). High-quality single crystals of C-Y_2O_3 can be grown, too. All these properties make the cubic R oxides attractive candidates for providing very stable and efficient host lattices for high-power solid-state laser applications.

The cubic C-type R sesquioxides are also well suited for use in systematic theoretical studies dealing with various luminescence phenomena since the cubic form extends over a wide host cation range, from R = Eu to Lu, Y, and Sc as well as In. The extended structural isomorphism gives the invaluable possibility to explore the evolution of many properties of different R^{3+} ions as dopants. A wealth of literature data about e.g. the energy level schemes is thus available [10, 11].

According to the latest crystal structure data available [12–14], the cubic C-type R oxides are isomorphic with the mineral bixbyite, $(Mn, Fe)_2O_3$ (space group $Ia3$, No 206, $Z = 16$ [15]). The R^{3+} ions occupy two sixfold-coordinated though distinctly non-equivalent sites with C_2 and S_6 point symmetries. The two sites differ from each other in the position of the R^{3+} ion relative to the oxygen vacancy (figure 1). In contrast to the case for the S_6 site, there is no centre of inversion symmetry in the C_2 site.

The presence of inversion symmetry in the R^{3+} site drastically affects the luminescence spectra of the R^{3+}-doped materials since in this case induced electric dipole transitions cannot gain intensity by the mixing of opposite parity electron configurations with the $4f^N$ one. The electric dipole transitions can occur only by weak vibronic coupling. The relatively weak magnetic dipole-induced transitions remain possible for ions residing in a site with inversion symmetry. However, the free ion selection rules strongly restrict the possible transitions of this type through the $\Delta J = 0, \pm 1$ (except for $0 \leftrightarrow 0$) rule. Only few pure magnetic dipole transitions are found in the R^{3+} spectra. The best examples can be found in the emission and absorption spectra of the Eu^{3+} ion (the $4f^6$ electron configuration). For Eu^{3+}-doped cubic C-R_2O_3, only a few lines are due to the Eu^{3+} ions in the S_6 sites, and practically all transitions usually observed originate from the Eu^{3+} ions in the C_2 sites. This leads to it being a very difficult task to determine the energy level scheme of the R^{3+} ions in the S_6 site.

The correct estimation of the energy level scheme of the Yb^{3+} ion is essential for the understanding of the spectroscopic properties of lasing materials. Many other important laser quantities depend also on the fine details of the local crystal fields (cfs) surrounding the Yb^{3+} ions in the host lattice. This paper is devoted to the study of the energy level scheme of the Yb^{3+} ions in the C$_2$ and S$_6$ sites in C-type R oxides. A further aim of the present work is to connect the estimation of the energy level scheme of the Yb^{3+} ion with the phenomenological cf simulation to the more accessible experimental energy level schemes for the Eu^{3+} ions in the C$_2$ and S$_6$ sites of the cubic C-type R$_2$O$_3$.

2. Experimental details

2.1. Sample preparation

The polycrystalline Eu^{3+}-doped yttrium oxide C-Y$_2$O$_3$ was prepared by heating the mixed R oxalate hydrate, (Y, Eu)$_2$(C$_2$O$_4$)$_3 \cdot x$H$_2$O, precipitates in air at 1100 °C for 4 h. For luminescence measurements the Y^{3+} host cation was partially replaced by a small amount of Eu^{3+} ions, nominally 2 mol%. The distribution of the dopant was assumed random and uniform which, however, does not completely exclude the statistical possibility of dopant pairs or higher associations. The samples were checked with routine x-ray powder diffraction analysis but no impurity phases or other anomalies were detected. The spectroscopic measurements revealed a complete solid solubility between the Eu^{3+} dopant and the Y^{3+} host cation.

2.2. Spectroscopic measurements

The luminescence of the Eu^{3+}-doped C-type Y$_2$O$_3$ was excited by a 200 W (OSRAM HBO) mercury lamp equipped with a wide-band filter providing global UV excitation around 300 nm. This wavelength region corresponds to the strong charge transfer absorption band of the Eu^{3+} ion. Different blue lines (454.4 and 457.9 nm) of a Spectra Physics 5 W continuous wave Ar$^+$-ion laser were used to excite the Eu^{3+} ion, too. Selective excitation at the ^{5}D$_0$ level of Eu^{3+} near 580 nm was carried out with a Spectra Physics 375/376 continuous wave rhodamine 6G dye laser. The emission attributed mainly to the ^{5}D$_0 \rightarrow {}^7$F$_{0-4}$ transitions was dispersed by a 1 m Jarrell-Ash single monochromator equipped with standard photomultiplier detection. All measurements were carried out at liquid nitrogen (77 K) and room temperatures (298 K). The resolution of the equipment was better than 1.0 cm^{-1}.

2.3. Energy level scheme calculations

The complex energy level schemes of the R^{3+} ions in the solid state result from several interactions—both within the 4f^N electron configuration and between the R^{3+} ion and its environment. Each interaction can be described with the aid of effective operators and their effect can be parametrized by using phenomenological models. The Coulombic interaction between the 4f electrons is described with the Slater integrals F^k ($k = 0, 2, 4,$ and 6) or Racah parameters E_k ($k = 0, 1, 2,$ and 3). The spin–orbit coupling (the coupling constant ζ_{4f}) splits the terms into the $^{2S+1}L_J$ states. α, β, and γ are the two-body electrostatic Trees parameters, and the T^k (Judd parameters) describe the corresponding three-body interactions. The effective Hamiltonian H_{FI} comprising these interactions can be written as follows:

$$H_{FI} = \sum_{k=0}^{3} E_k(nf, nf)e^k + \zeta_{4f}A_{SO} + \alpha L(L+1) + \beta G(G_2) + \gamma G(R_7) + \sum_{k=2,3,4,6,7,8} T^k t_k \quad (1)$$

where the angular parts e^k, A_{SO}, L, $G(G_2)$, $G(R_7)$, and t_k have their usual meanings [16, 17]. Higher-order magnetic spin–spin and spin–other-orbit interactions as well as the

electrostatically correlated spin–orbit interactions can be parametrized by Marvin integrals M^k ($k = 0, 2$, and 4) and P^k ($k = 2, 4$, and 6), respectively.

When the R^{3+} ion is introduced into a solid it experiences an inhomogeneous electrostatic field produced by the surrounding charge distribution. The cf Hamiltonian H_{CF} can be obtained as follows [16]:

$$H_{CF} = \sum_k \sum_{q=-k}^{q=k} \{B_q^k [C_q^k + (-1)^q C_{-q}^k] + iS_q^k [C_q^k - (-1)^{-q} C_{-q}^k]\} \tag{2}$$

where the parameters B_q^k and S_q^k are the coefficients of the cf expansion, i.e. the real and imaginary functions of the radial distances, respectively. The C_q^k are tensor operators of rank k closely related to the spherical harmonics.

The phenomenological simulation of the cf energy level scheme of the R^{3+} ions involves the determination of a large number of parameters (even more than 30) from the experimentally determined energy level scheme. For the two R^{3+} ions, Eu^{3+} and Yb^{3+}, dealt with in this study, the situation is quite different. For the Yb^{3+} ion with the $4f^{13}$ electron configuration, only one free ion parameter, the spin–orbit coupling constant ζ_{4f}, must be determined from the experimental data. A value of 2897 cm^{-1} was used in all the calculations for Yb^{3+}.

The $4f^6$ electron configuration of the Eu^{3+} ion is very complex with up to 3003 cf levels. The simulation of the cf effect is usually carried out by using the 49 cf levels of the ground term, the ^7F_J ($J = 0$–6) septet only. This drastic truncation can be justified by the weak mixing of the ground septet with the rest of the $4f^6$ configuration, but it may lead to erroneous positions of the ^7F_J level barycentres. This problem was partially dealt with earlier [18] but in spite of the pitfalls involved this method of simulation was used in this work, too.

The best-fit set of the cf parameters was obtained through minimizing the rms function σ between the observed and calculated energy level values with the standard least-squares refinement by using the program IMAGE [19].

3. Results and discussion

3.1. Energy level scheme of Eu^{3+} in the S_6 site

The overwhelming majority of the spectroscopic investigations on the cubic C-type R sesquioxides, C-R_2O_3, have dealt with the spectroscopic properties of the R^{3+} ions in the low-symmetry C_2 site [10, 11]. While still concentrating on the main site (the C_2 sites— 24—are three times more frequent than the S_6 sites—8—in the unit cell of C-R_2O_3), some investigations have dealt also with the properties of the S_6 site [20–24]. Several spectral lines were assigned [20] as originating from the Eu^{3+} ions in the S_6 site of the cubic C-Y_2O_3: two in absorption, corresponding to the $^7F_0 \rightarrow {}^5D_1$ transition, and two in emission, corresponding to the $^5D_0 \rightarrow {}^7F_1$ transition. Monitoring the evolution of the intensity of the $^7F_1 \rightarrow {}^5D_0$ transition at 17 170 cm^{-1} in absorption as a function of temperature, the $^7F_0 \rightarrow {}^7F_1$ energy difference was determined and eventually the $^5D_0$ level position was derived to be at 17 302 cm^{-1}.

The present study carried out on the luminescence of the Eu^{3+}-doped C-R_2O_3 series under Ar^+ laser excitation at 454.5 nm confirmed in principle the results of the previous study [20]. A similar emission spectrum for the polycrystalline Y_2O_3:Eu^{3+} sample was observed for the Eu^{3+} ions residing in the S_6 site. The spectroscopic results of the present study and those found in the literature [20–23] together with the deductions on the energy level scheme are compiled into tables 1 and 2. The results from different sources seem to be in rather good agreement—but only as far as the energy level positions are concerned. Since the polarization measurements of spectral lines are practically the only reliable ones to indicate the correct level assignments,

Table 1. Electronic transitions in the spectra of the Eu^{3+} ions in the S_6 point site in cubic C-Y_2O_3.

Transition	Energy (cm^{-1})			
	[20]	[21]	[22]	This work
$^7F_0 \rightarrow {}^5D_1$	19 080			
$^7F_0 \rightarrow {}^5D_1$				18 996[a]
$^5D_1 \rightarrow {}^7F_0{}^a$	18 991		18 997	
$^5D_1 \rightarrow {}^7F_2{}^a$				18 157[a]
$^7F_0 \rightarrow {}^5D_0$	17 302			
$^5D_0 \rightarrow {}^7F_1$	17 170	17 176	17 176	17 177
	16 873	16 863	16 869	16 880
Vibronics		16 793		16 829
				16 775

[a] Lines observed only in the emission spectra.

Table 2. Experimental and calculated $^5D_{0,1}$ and $^7F_{0-2}$ energy level schemes of the Eu^{3+} ions in the S_6 site in cubic C-Y_2O_3.

$^{2S+1}L_J$ level	Energy (cm^{-1})			
	[20]	[23]	Experimental	Calculated[a]
$^5D_1$	19 080 (A)			
$^5D_1$	18 991 (E)		18 996 (A)	
$^5D_1$ barycentre	19 021			
$^5D_0$	17 302 (A)			
$^7F_1$	132 (E)		125 (A)	126 (A)
$^7F_1$	429 (A)		448[b] (E)	447[b] (E)
$^7F_1$ barycentre	231		340	340
$^7F_2$		830 (E)	839	821 (E)
		948 (E)		955 (A)
		1184 (A)		1190 (E)
$^7F_2$ barycentre		948		995

[a] Calculated with the crystal field parameters from table 3.
[b] Mean value.

those deduced from measurements on powder samples are left always with some uncertainty. Accordingly, the present study gives assignments different from the previous ones [20, 23].

The method used here to obtain the level assignments needs some explanation. Given that all the other facts are similar, the level assignments affect the energy position of the barycentre of each $^{2S+1}L_J$ level. The energy gaps between the barycentres depend practically exclusively on the strength of the spin–orbit coupling since this interaction acts only within a given ^{2S+1}L term [18]. However, this may be true only when the wavefunctions of the levels are pure enough in the original term, i.e. when the quantum number J is low in the case of the Eu^{3+} ion. For levels with high J-values, the J-mixing becomes more important—especially when the cf effect is strong—and the present method may not be applicable [25]. The level assignments to be carried out in this work fulfil the necessary requirement: the levels belong either to the ^5D or ^7F term with low J-values, i.e. from 0 to 2, since no experimental data are available for higher J-levels. Moreover, the ^7F term is the only one in the $4f^6$ electron configuration and thus the effects of additional interactions mixing the wavefunctions are minimized.

The cf level assignments for the $^5D_1$ and $^7F_{1-2}$ levels can thus be carried out with high reliability. Both the $^5D_1$ and $^7F_1$ levels are split in the cf of S_6 symmetry into two crystal field
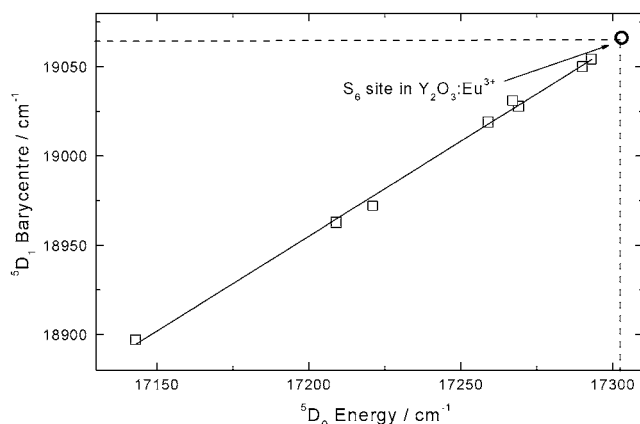
Figure 2. $^5D_1$ barycentre energy as a function of the $^5D_0$ level energy of the Eu^{3+} ion in various host lattices.

levels: one singlet (A) and one doublet (E) [10]. Following the procedure published earlier [18] then applied for the $^7F_1$ barycentre, the barycentre of the $^5D_1$ levels may be presented as a function of the $^5D_0$ level energy (figure 2) for a number of different Eu^{3+}-doped compounds. If we adopt the $^5D_0$ level position at 17 302 cm^{-1} [20] for the C-type Y_2O_3, the barycentre of the two $^5D_1$ cf levels should then be found at 19 060 cm^{-1} (figure 2). However, following the original level assignments [20], i.e. 18 991 and 19 080 cm^{-1} for the E and A levels, respectively, the barycentre of the $^5D_1$ level is at 19 022 cm^{-1} which is clearly too low a value. The original level assignment [20] for the $^5D_1$ level should be reversed, i.e. with the doublet as the higher and the singlet as the lower cf level, since the recalculated barycentre energy at 19 053 cm^{-1} is then close to the expected value (19 060 cm^{-1}).

The cf level assignments for the $^5D_1$ and $^7F_1$ levels should be the same if both level splittings are significantly different from zero because the cf splittings are controlled by the same cf parameters. Moreover, on the basis of both theoretical considerations and experimental energy level simulations, the $^7F_1$ barycentre energy is in the range from 340 to 380 cm^{-1} [10, 18]. If we consider the upper $^7F_1$ component as E and the lower as A, the $^7F_1$ barycentre is situated close to the correct range, at 340 cm^{-1} instead of 231 cm^{-1} obtained in the earlier study [20]. Previous work on the phenomenological simulation of the energy level scheme of Gd^{3+} in C-Y_2O_3 [26] as well as the semi-empirical calculations [24] on the Eu^{3+} ion in the two sites in C-Y_2O_3 support the present level assignment, i.e. 125 (A) and 448 cm^{-1} (E).

In order to complete the build-up of the experimental energy level scheme with the $^7F_2$ cf level for the S_6 site, the data concerning some extra lines found in the Raman spectra of C-Y_2O_3:Eu^{3+} [23] are reanalysed. Since the $^7F_2$ level is split in the crystal field of S_6 symmetry into one singlet (A) and two doublet (E) cf levels, the extra lines were originally assigned to the electronic cf levels of the $^7F_2$ level as follows: 830 (E), 948 (E), and 1184 cm^{-1} (A). This assignment gives the $^7F_2$ barycentre energy as 948 cm^{-1}. As shown for the $^7F_1$ level, this assignment is not necessarily a true one. Accordingly, the previous level assignments were verified by using the procedure based on a relationship between the barycentre energies of the $^7F_1$ and $^7F_2$ levels (figure 3). In contrast to the relationship between the $^5D_0$ level position and the $^5D_1$ barycentre energy, the present relationship is much less smooth. The discrepancies may be taken as an indication of the effect of the J-mixing due to the cf interaction [25]. However, an approximate value of 1018 cm^{-1} can be deduced for the $^7F_2$ barycentre, which is in good agreement with the following cf level reassignment: 830 (A), 948 (E), and 1184 (E).
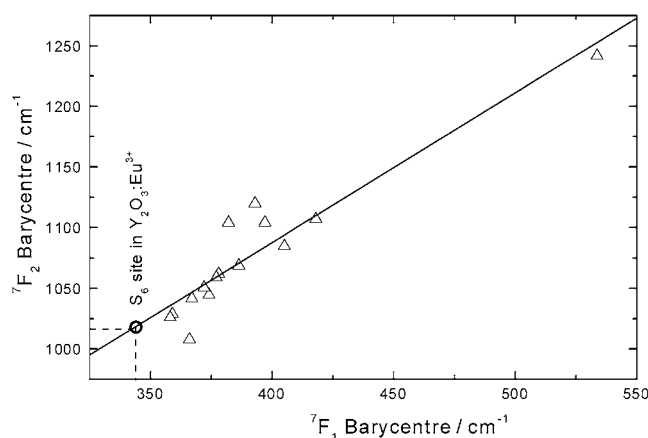
Figure 3. $^7F_2$ barycentre energy as a function of the $^7F_1$ barycentre of the Eu^{3+} ion in various host lattices.

The analysis of the ^7F energy level scheme of the Eu^{3+} ion in the S$_6$ site of C-Y$_2$O$_3$ could not be continued any further, since no data are available for the $^7F_{3-6}$ cf levels. The lack of data is probably due to the weakness and/or the low purity of the magnetic dipole transitions, e.g. the $^5D_2 \rightarrow {}^7F_3$ and $^5D_3 \rightarrow {}^7F_4$ transitions which should give the information needed.

3.2. Crystal field calculations for Eu^{3+} in the S$_6$ site

Despite the relatively high point symmetry (S$_6$) of the Eu^{3+} ion in C-R$_2$O$_3$, the cf expansion contains a high number of terms, in total nine cf parameters including both six real (B_0^2, B_0^4, B_3^4, B_0^6, B_3^6, and B_6^6) and three imaginary parts (S_3^4, S_3^6, and S_6^6) [10]. Taking into account the number of energy levels available—in general for the S$_6$ symmetry and especially for the Eu^{3+} in C-Y$_2$O$_3$—the full phenomenological cf simulation is clearly impossible. However, there exists an *a priori* calculation concerning the cf parameters for Eu^{3+}-doped C-Y$_2$O$_3$ [24] which, taking into account the inherent limitations of such calculations, can give reliable values for the sixth-rank and, to a certain extent, for the fourth-rank parameters, too. The second-rank parameter values are still better obtained from experimental data. These restrictions are well suited to the Eu^{3+}-doped C-Y$_2$O$_3$ case since reliable experimental data are available for the cf splitting of both the $^7F_1$ and $^7F_2$ levels, which yield in a quite straightforward manner the second- and fourth-rank parameter values. More supporting experimental data are available from the analysis of the cf splitting of the four $^6P_{7/2}$ levels of the Gd^{3+} ion in the S$_6$ site of C-Y$_2$O$_3$ [26]. The cf splittings of both the $^6P_{7/2}$ and $^7F_1$ levels of Gd^{3+} and Eu^{3+}, respectively, depend almost exclusively on the second-rank parameter values because the fourth- and sixth-rank reduced matrix elements are very small or zero for these levels. The B_0^2-parameter value was found to be negative and thus the value of the B_0^2-parameter is now defined unambiguously.

The cf effect on the $^7F_1$ and $^7F_2$ levels of Eu^{3+} in the S$_6$ site was simulated by using the cf parameters from [24] as the starting set. The best-fit set of cf parameters (table 3) simulated the experimental energy level scheme well, as is revealed by the calculated energy levels with irreducible representations (table 2). The $^7F_2$ barycentre energy obtained from the computed levels is 995 cm^{-1} which is close to the value deduced from the experimental data for a set of Eu^{3+}-doped compounds (figure 3), and thus the present level assignments for the $^7F_2$ cf components can now be considered correct.

Table 3. Crystal field parameters for the Eu^{3+} and Yb^{3+} ions in the S_6 and C_2 sites of the cubic C-Y_2O_3. (Values in square brackets were kept fixed in refinements.)

Parameter	Parameter value (cm^{-1})		
	C-Y_2O_3 S_6 site		C-Y_2O_3 C_2 site
	Refined for Eu^{3+}	40% reduced from Eu^{3+}	Extrapolated for Yb^{3+} [11]
B_0^2	−1486	−892	−225
B_2^2			−618
B_0^4	−1248	−749	−1226
B_2^4			−1012
S_2^4			324
B_3^4	−2346	−1407	
S_3^4	[267][a]	160	
B_4^4			736
S_4^4			−832
B_0^6	[734][a]	440	177
B_2^6			284
S_2^6			112
B_3^6	[361][a]	217	
S_3^6	[−33][a]	−20	
B_4^6			62
S_4^6			−159
B_6^6	[567][a]	340	−27
S_6^6	[−57][a]	−34	−20
N_V	4969	2980	3318
Levels	6		
σ	7.5		

[a] From [24].

3.3. Energy level scheme of Yb^{3+} in the S_6 site

The previous, incorrect level assignments obtained for the Eu^{3+}-doped C-Y_2O_3 [20, 23, 27] will inevitably lead to incorrect calculated cf splittings of the $^2F_{7/2}$ and $^2F_{5/2}$ levels of Yb^{3+} in the S_6 site of C-R_2O_3. The prediction of the splitting of the two ^2F levels of Yb^{3+} in the S_6 site of C-R_2O_3 will be carried out by using the following two basic ideas:

 (a) evolution of the cf strength along the lanthanide series [28, 29]; and
 (b) the relationship between the $^2F_{7/2}$ and $^2F_{5/2}$ barycentre energies together with some energy level data reported previously [4, 18].

The cf strength in any host can be described the parameter N_V [30]:

$$N_V = \left[\sum_{k,q} \left(\frac{4\pi}{2k+1} \right) |B_q^k|^2 \right]^{1/2}. \tag{3}$$

The N_V-value decreases with decreasing ionic radius of the dopant if the dopant is embedded in the same host lattice [28, 29], as shown for the R^{3+} doped in the C_2 site of Y_2O_3 (figure 4).
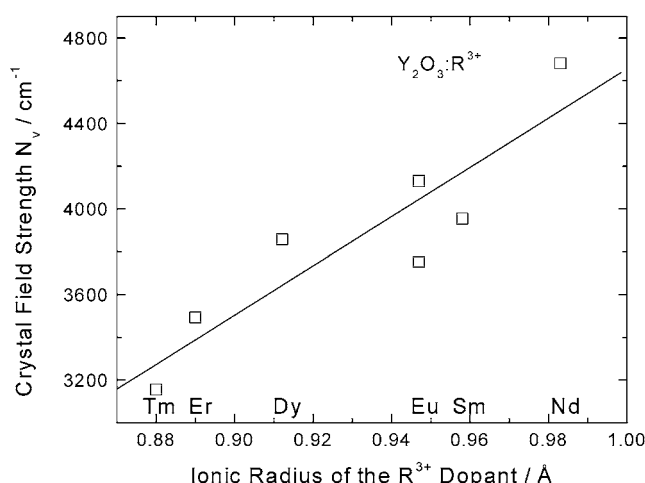
Figure 4. Crystal field strength parameter, N_V, as a function of the ionic radius of the dopant in the R^{3+}-doped cubic C-Y_2O_3 series (C_2 site).

The individual cf parameter values [10, 11, 31] follow the evolution of the N_V-value, at least in the Y_2O_3:R^{3+} series.

The evolution of the cf B_q^k-parameter values as a function of the host cation can be divided into two parts:

(a) the evolution of the radial integrals $\langle r^k \rangle$; and
(b) the evolution of the values of the lattice sum parameter A_q^k:

$$B_q^k = \tau^{-k}(1 - \sigma_k)A_q^k \langle r^k \rangle \tag{4}$$

where the factors τ and σ_k describe the expansion of the 4f wavefunctions in the solid state and the shielding effect of the outer electrons, respectively. The increase in the values of the lattice sum parameter A_q^k is more than compensated by the decrease in the values of the radial integral $\langle r^k \rangle$, resulting in an overall decrease in the cf B_q^k-parameter values from the cerium to the ytterbium host. Experimentally, this has been verified both for the ROCl [31] and $R_3Ga_5O_{12}$ [28] series, but this evolution for the C-R_2O_3 series cannot be verified because of the lack of experimental data (see e.g. [10]).

The N_V-value is reduced by $\approx 25\%$ from europium to ytterbium in the Y_2O_3:R^{3+} series (figure 4). A further decrease can be expected with decreasing size of the host cation, e.g. from Y_2O_3 to Sc_2O_3, in accordance with the electrostatic point charge model (equation (4)), but the exact amount of this decrease cannot be verified due to the evident lack of experimental data (Y^{3+} and Sc^{3+} have no nf energy levels to study). The exact estimation is further made more difficult because of the local distortions created by the introduction of the dopant with different size to the host cation [28]. Using the relationship between the total cf splitting of the $^{2S+1}L_J$ level and the N_V-value [30, 32], the amount of the modification of the cf parameters was established by comparison between the experimental and calculated cf splittings of the $^2F_{7/2}$ level of Yb^{3+} in the S_6 site of C-Sc_2O_3 (figure 5). Yb^{3+}-doped C-Sc_2O_3 was chosen as a point of reference since enough experimental data were available for this system. In total, a decrease of around 40% in the cf parameters (and in the N_V-value) was obtained from C-Y_2O_3:Eu^{3+} to C-Sc_2O_3:Yb^{3+} (table 3). The cf splitting of the $^2F_{7/2}$ level of the Yb^{3+} ion in the S_6 site of
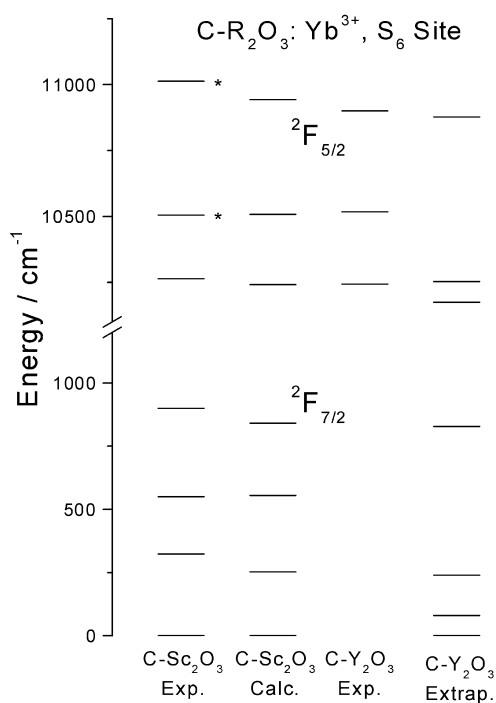
Figure 5. Crystal field splitting of the $^2F_{5/2}$ and $^2F_{7/2}$ levels of the Yb^{3+} ions in the S$_6$ site of the cubic C-Sc$_2$O$_3$. The levels marked with $*$ were deduced from the overall splitting and barycentre position of the $^2F_{5/2}$ level. The calculated scheme was obtained with the reduced cf parameters (table 3). The $^2F_{7/2}$ scheme was calculated using the cf parameters extrapolated from the C-Y$_2$O$_3$:R^{3+} series [27].

C-Sc$_2$O$_3$ calculated by using the reduced values of the cf parameters for C-Y$_2$O$_3$:Eu^{3+} indicates a good agreement between the experimental and calculated energy level schemes (figure 5).

In order to find the cf splitting of the excited $^2F_{5/2}$ level of the Yb^{3+} ion in the S$_6$ site of C-Sc$_2$O$_3$ a procedure quite similar to that used previously in section 3.1 was employed. The site-selective excitation spectra of Yb^{3+} in cubic C-R$_2$O$_3$ [33, 34] have shown clearly that the C$_2$ and S$_6$ sites possess two non-similar energy schemes for the ground $^2F_{7/2}$ level. The energies of the four cf components of the $^2F_{7/2}$ level for the S$_6$ site in C-Sc$_2$O$_3$ are 0, 323, 550, and 900 cm^{-1} [34], while the lowest $^2F_{5/2}$ level is at 10 260 cm^{-1} [35]. As the overall cf splitting of the ground level is known (900 cm^{-1}), the overall splitting of the excited level $^2F_{5/2}$ can be deduced to be about 750 cm^{-1} (figure 6) and thus the highest cf level is at 11 010 cm^{-1}. The last step is to find the missing third cf level of the $^2F_{5/2}$ manifold. Since all the four cf levels of the ground $^2F_{7/2}$ level are known, it is possible to deduce the barycentre of the $^2F_{5/2}$ level (figure 7) to be at 10 593 cm^{-1}, corresponding to the barycentre of $^2F_{7/2}$ at 443 cm^{-1}. The third $^2F_{5/2}$ level must thus be at 10 505 cm^{-1}.

The comparison of the predicted and calculated $^2F_{7/2}$ and $^2F_{5/2}$ energy level schemes for Yb^{3+} in the S$_6$ site of C-Sc$_2$O$_3$ yielded surprisingly good results (figure 5). The two sets of cf splittings for both free ion levels were very similar (the experimental values are in parentheses): 0 (0), 253 (323), 551 (550), and 840 (900) cm^{-1} for the $^2F_{5/2}$ level and 102 43 (10 260), 10 503 (10 505), and 10 941 (11 010) cm^{-1} for the $^2F_{5/2}$ level. The results obtained indicate that the method used to predict the $^2F_{5/2}$ cf level scheme is reliable.
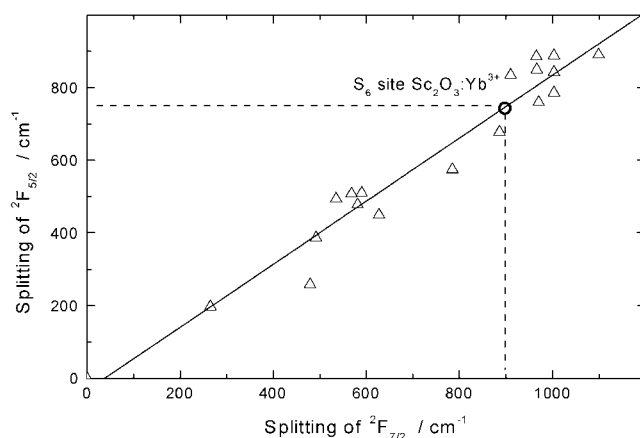
Figure 6. The relationship between the overall splitting of the $^2F_{5/2}$ and $^2F_{7/2}$ levels for various Yb^{3+}-doped compounds.

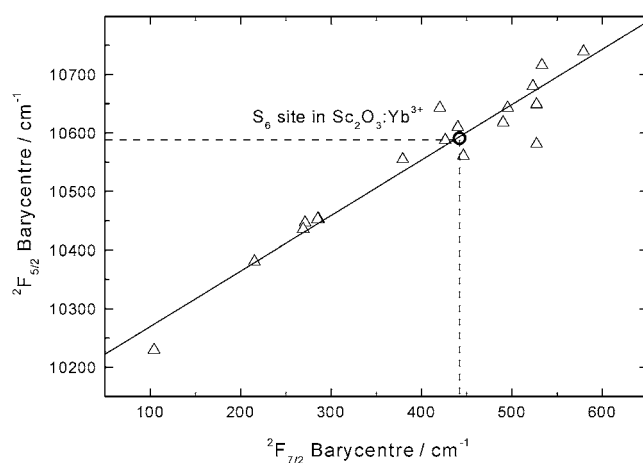**Figure 7.** $^2F_{5/2}$ barycentre energy as a function of the $^2F_{7/2}$ barycentre for various Yb^{3+}-doped compounds.

In contrast to the C-Sc$_2$O$_3$:Yb^{3+} case where the cf splitting of the ground level is known [34], only the excited $^2F_{5/2}$ level scheme of C-Y$_2$O$_3$:Yb^{3+} has been determined experimentally [35, 36]. The absorption line at $10\,517\,\mathrm{cm}^{-1}$ has been assigned to the S$_6$ site of Yb^{3+} and the highest $^2F_{5/2}$ sublevel is situated at about $10\,900\,\mathrm{cm}^{-1}$ [36]. The lowest $^2F_{5/2}$ cf level seems to be at $10\,243\,\mathrm{cm}^{-1}$ [35]. The experimental $^2F_{5/2}$ level scheme of Yb^{3+} in C-Y$_2$O$_3$ is thus $102\,43$–$10\,517$–$10\,900\,\mathrm{cm}^{-1}$, while that calculated by using the reduced cf parameters (table 3) is $10\,243$–$10\,503$–$10\,941\,\mathrm{cm}^{-1}$ (figure 5). The agreement between the experimental and calculated cf splittings of the $^2F_{5/2}$ level is rather good. The differences underline the fact that the cf effect is stronger in the C-Sc$_2$O$_3$ than in the C-Y$_2$O$_3$ host. The last $^2F_{5/2}$ energy level scheme in figure 5 obtained by using the extrapolated cf parameters [27] is different to the others. The reason for this is—at least partly—the B_0^2-parameter, which was deduced to be positive [27] in contradiction to the present work as well as the literature values [24].
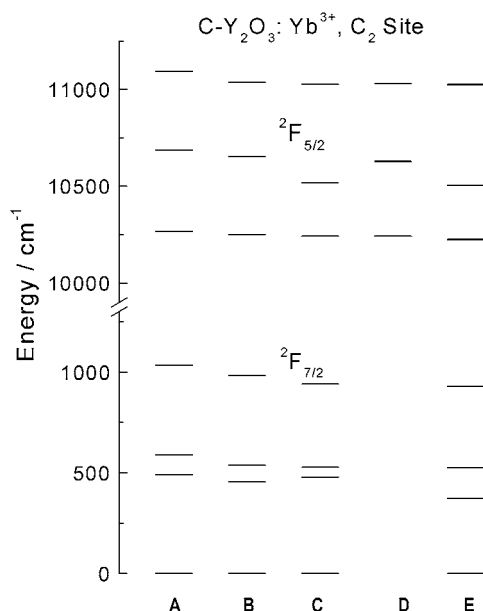
Figure 8. Calculated and experimental cf splittings of the $^2F_{5/2}$ and $^2F_{7/2}$ levels of the Yb^{3+} ions in the C$_2$ site of C-Y$_2$O$_3$: (A) calculated with the cf parameters [35], (B) calculated with the extrapolated cf parameters [11], (C) experimental data [35], (D) from absorption spectra [35], (E) experimental data [37].

3.4. Energy level scheme of Yb^{3+} in the C$_2$ site

As the final part of the present work, the energy level scheme for the Yb^{3+} ion in the C$_2$ site of C-Y$_2$O$_3$ was investigated by using the procedures described above. Different energy level schemes have been obtained experimentally and by calculations (figure 8). Schemes A and B are those calculated by using the cf parameters [36] and the extrapolated cf parameters [11], respectively, while scheme C has been obtained experimentally [35]. In general, the results are rather similar and the individual cf splittings of both levels are reproduced rather well, though the calculated overall splittings of the ground level seem to be slightly too large. The experimental data give the overall cf splittings of 941 and 784 cm^{-1} for the $^2F_{7/2}$ and $^2F_{5/2}$ levels, respectively. These values are confirmed by the literature data (figure 6) which means that the lowest and the highest cf levels of the experimental data [35] are correctly chosen for both levels.

The experimental $^2F_{7/2}$ barycentre is at 487 cm^{-1}, which corresponds to 10 636 cm^{-1} for the $^2F_{5/2}$ barycentre (figure 7). However, the experimental $^2F_{5/2}$ barycentre at 10 596 cm^{-1} is in disagreement with the predicted value. One of the cf levels of the $^2F_{5/2}$ level is thus incorrect and since the overall splittings were found correctly it is most probably the middle Stark level. According to predictions, the incorrect (or missing) cf level should be at 10 635 cm^{-1}. This statement is supported by scheme D which corresponds to the experimental data (10 243, 10 629, and 11 030 cm^{-1}) reported for the C$_2$ site in C-Y$_2$O$_3$:Yb^{3+} [36]. The last experimental energy level scheme E is similar to C as far as the excited $^2F_{5/2}$ level is concerned, but the ground $^2F_{7/2}$ level scheme is slightly different.

4. Conclusions

Reliable energy level schemes of the Yb^{3+} ions embedded in various crystalline matrices are difficult to establish experimentally due to the presence of vibronic lines—both in the absorption and emission spectra. However, the knowledge of the cf level energies of the $^2F_{7/2}$ and $^2F_{5/2}$ free ion levels is very important for the understanding of the different processes involved, e.g. in the new DPSSLs. In the present study a method was presented for establishing the energy levels of the Yb^{3+} ion in both the C_2 and S_6 sites of cubic C-type R oxides. The S_6 site of cubic $C-RE_2O_3$ presents a very complicated case due to a very restricted amount of experimental energy level information due to the selection rules for a point site which possesses an inversion centre.

The energy level schemes as well as the corresponding cf parametrization analyses for the Eu^{3+} and Yb^{3+} ions embedded in both the C_2 and S_6 sites were studied in detail and several modifications were suggested. The present results give a more reliable interpretation of the energy level schemes and are, moreover, in agreement with the literature data.

This approach has now been successfully applied to the interpretation of the spectra and energy level schemes of the Pr^{3+}, Nd^{3+}, Eu^{3+} [18], and Yb^{3+} ions in various host lattices. The utility of the methods presented in this work is evident and they should be adopted by all researchers working with R spectroscopy in order to solve spectroscopic puzzles due to lines of vibronic or impurity origin.

Acknowledgment

References

[1] Krupke W F 2000 *IEEE J. Sel. Top. Quantum Electron.* **6** 1287
[2] Druon F, Chenais S, Raybaut P, Balembois F, Georges P, Gaume R, Aka G, Viana B, Mohr S and Kopf D 2002 *Opt. Lett.* **27** 197
[3] Haumesser P H, Gaume R, Viana B, Aka G, Vivien D and Ferrand B 2001 *Trends Opt. Photon.* **50** 425
[4] Haumesser P H, Gaume R, Viana B, Antic-Fidancev E and Vivien D 2001 *J. Phys.: Condens. Matter* **13** 5427
[5] Lebedev V A, Voroshilov I V, Ignatiev B V, Gavrilenko A N, Isaev V A and Shestakov A V 2000 *J. Lumin.* **92** 139
[6] Druon F, Balembois F, Georges P, Brun A, Courjaud A, Honninger C, Salin F, Aron A, Mougel F, Aka G and Vivien D 2000 *Opt. Lett.* **25** 423
[7] Wang P, Dawes J M, Dekker P and Piper J A 2000 *Opt. Commun.* **174** 467
[8] Peters V, Mix E, Fornasiero L, Petermann K, Huber G and Basun S A 2000 *Laser Phys.* **10** 417
[9] Blasse G and Grabmaier B C 1994 *Luminescent Materials* (Berlin: Springer)
[10] Görller-Walrand C and Binnemans K 1996 Rationalization of crystal-field parametrization *Handbook of the Physics and Chemistry of Rare Earths* vol 23, ed K A Gschneidner Jr and L Eyring (Amsterdam: Elsevier) ch 155
[11] Morrison C A and Leavitt R P 1982 Spectroscopic properties of triply ionized lanthanides in transparent host crystals *Handbook of the Physics and Chemistry of Rare Earths* vol 5, ed K A Gschneidner Jr and L Eyring (Amsterdam: North-Holland) ch 46
[12] Faucher M and Pannetier J 1980 *Acta Crystallogr.* **36** 3209
[13] Marezio M 1966 *Acta Crystallogr.* **20** 723
[14] Fert A 1962 *Bull. Soc. Fr. Minéral. Cristallogr.* **85** 267
[15] Lonsdale K (ed) 1962 *International Tables for X-ray Crystallography* vol 3 (Birmingham: Kynoch) p 163
[16] Wybourne B G 1965 *Spectroscopic Properties of Rare Earths* (New York: Interscience) ch 6
[17] Judd B R, Crosswhite H M and Crosswhite H 1968 *Phys. Rev.* **169** 130
[18] Antic-Fidancev E 2000 *J. Alloys Comp.* **300/301** 2

[19] Porcher P 1989 *Computer Program IMAGE for the Simulation of d^N and f^N Configurations Involving the Real Crystal Field Parameters (CNRS, Meudon, France, 1989)* (unpublished)
[20] Heber J, Hellwege K H, Köbler U and Murmann H 1970 *Z. Phys.* **237** 189
[21] Tola P, Dexpert-Ghys J, Lemonier M, Retournard A, Pagel M and Goulon J 1983 *Chem. Phys.* **78** 339
[22] Su Q, Barthou C, Denis J P, Pelle F and Blanzat B 1983 *J. Lumin.* **28** 1
[23] Schaak G and Koningstein J A 1970 *J. Opt. Soc. Am.* **60** 1110
[24] Faucher M and Dexpert-Ghys J 1981 *Phys. Rev.* B **24** 3138
[25] Görller-Walrand C, Huygen E, Binnemans K and Fluyt L 1994 *J. Phys.: Condens. Matter* **6** 7797
[26] Antic-Fidancev E, Lemaître-Blaise M and Caro P 1982 *J. Chem. Phys.* **76** 2906
[27] Gruber J, Leavitt R P, Morrison C and Chang N C 1985 *J. Chem. Phys.* **82** 5373
[28] Antic-Fidancev E, Hölsä J, Lastusaari M and Lupei A 2001 *Phys. Rev.* B **64** 195108
[29] Antic-Fidancev E, Hölsä J and Lastusaari M 2002 *J. Alloys Compounds* **341** 82
[30] Auzel F and Malta O L 1983 *J. Physique* **44** 201
[31] Hölsä J, Lamminmäki R-J, Lastusaari M, Porcher P and Sáez Puche R 2000 *J. Alloys Compounds* **300/301** 45
[32] Malta O L, Antic-Fidancev E, Lemaître-Blaise M, Taibi M and Milicic-Tang A 1995 *J. Alloys Compounds* **228** 41
[33] Petermann K, Huber G, Fornasiero L, Kuch S, Mix E, Peters V and Basun S A 2000 *J. Lumin.* **87–89** 973
[34] Petermann K, Fornasiero L, Mix E and Peters V 2002 *Opt. Mater.* **19** 67
[35] Mix E 1999 *Dissertation* Hamburg University (Aachen: Shaker) (ISBN 3-8265-6686-6)
[36] Chang N C, Gruber J, Leavitt R P and Morrison C 1982 *J. Chem. Phys.* **76** 3877
[37] Laversenne L, Guyot Y, Goutaudier C, Cohen-Adad M T and Boulon G 2001 *Opt. Mater.* **16** 475